a promising candidate for the delivery of anticancer drugs to cancer cells.

It has been demonstrated that various factors affect the transport activity of PEPT1 [6]. For example, PEPT1 is regulated by pharmacological agents, such as anticancer drugs, 5-fluorouracil (5-FU) [7] and cyclophosphamide [8], an agonist for α_2-adrenergic receptor, clonidine [9], and a selective σ-receptor ligand, pentazocine [10]. However, there is little information about the regulation of human PEPT1 in cancer cells. Elucidation of the regulation of human PEPT1 in cancer cells by anticancer drugs may be essential for developing a drug delivery system targeting PEPT1.

Gastric cancer is one of the most frequent cancer in the world. The characterization of the cellular pathophysiology of gastric cancers is important for diagnosis, treatment and prevention, and numerous studies about gene expression profiles of gastric cancer have been performed [11,12]. However, the expression and functional characterization of PEPT1 in gastric cancer cells have not been clarified. In the present study, therefore, we examined the expression and function of PEPT1 in the gastric cancer cell line MKN45. Furthermore, the effects of 5-FU and cisplatin (CDDP) on PEPT1 and, as a comparison, those on facilitative glucose transporter 1 (GLUT1) were examined in MKN45 cells. Both drugs are frequently used for treating advanced gastric cancer.

2. Materials and methods

2.1. Agents

[^{3}H]Glycylsarcosine and 2-deoxy-D-[^{3}H]glucose were purchased from Moravek (Mercury Lane, Brea, CA) and Amersham (Buckinghamshire, England), respectively. Ceftibuten and cephalexin were kindly provided by Sionogi and Co. (Osaka, Japan). Cefadroxil was from Bristol Meyers Co. (Tokyo, Japan). Cyclacillin and cefotiam were from Takeda Chemical Industries (Osaka, Japan). Valacyclovir was from GlaxoSmithKline Research and Development (Hertfordshire, UK). Bestatin was from Nippon Kayaku (Tokyo, Japan). Glycine and 5-fluorouracil were obtained from Nacalai Tesque, Inc. (Kyoto, Japan). Glycylsarcosine, ampicillin and cisplatin were purchased from Sigma Chemical Co. (St Louis, MO). All other chemicals used were of the highest purity available.

2.2. Gastric cancer cell lines

The human gastric cancer cell line MKN45 was obtained from Health Science Research Resources Bank (Osaka, Japan). MKN45 cells were cultured at 37 °C in a humidified atmosphere of 5% CO_2 and 95% air and maintained in RPMI-1640 medium containing 10% fetal bovine serum. The cells were subcultured every 5–6 days using 0.02% EDTA and 0.05% trypsin, and medium was replaced every 2–3 days. Typically, the cells cultured for 6 days were used for uptake studies and expression analysis.

2.3. mRNA expression analysis

Total RNA was isolated from MKN45 cells using an RNeasy mini kit (Qiagen, Hilden, Germany) according to the manufacturer's instructions. The RNA was reverse-transcribed using SuperScript™II RT (Invitrogen, Grand Island, NY) and amplified using Taq DNA polymerase (TaKaRa, Otsu, Japan) and PEPT1-specific oligonucleotide primers. The primer sequences for PEPT1 (accession number NM_005073) were as follows: forward, 5′-ACACAGTTTCTTT-GGTTATCCC-3′(74–95 bp); reverse, 5′-ATGA-GAGCAGGAGGAACCCCAA-3′ (661–682 bp). PCR reaction was performed as follows: after an initial denaturation at 95 °C for 1 min, followed by 35 cycles of 95 °C for 1 min, 55 °C for 1 min, and 72 °C for 1 min, and a final elongation at 72 °C for 10 min.

For quantification of the amounts of PEPT1, GLUT1 and GAPDH mRNA expression, the real-time PCR method was carried out using the ABI PRISM 7700 sequence detector (Applied Biosystems, Foster, CA). The primer-probe set used for PEPT1 was as follows: forward primer, 5′-ATTGTGTCG CTCTCCATTGTCTAC-3′ (306–329 bp); reverse primer, 5′-ATGACCTCACAGACCACAACCAT-3′ (367–389 bp); fluorescence probe, 5′-(6-Fam) TTGGACAAGCAGTCACCTCAGTAAGCTCCA (Tamra) (phosphate)-3′ (334–363 bp). The primer-probe sets used for GLUT1 and GAPDH were Pre-developed TaqMan Assay Reagents

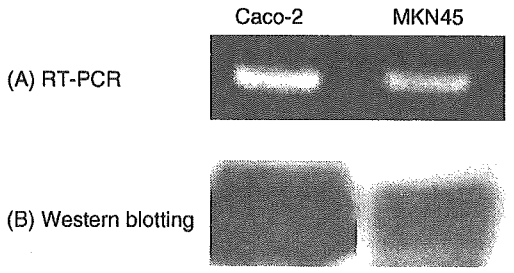

Fig. 1. PEPT1 mRNA (A) and protein (B) expression in MKN45 cells. As a positive control, Caco-2 cells on day 14 were used. (A) Total RNA (1 μg) extracted from MKN45 or Caco-2 cells was reverse-transcribed and detected with specific oligonucleotide primers. (B) Crude membranes (70 μg) from MKN45 cells and brush-border membranes (20 μg) from Caco-2 cells were prepared and PEPT1 protein expression was detected by Western blotting using PEPT1-specific antibody.

(Applied Biosystems), and the reactions were performed according to the manufacturer's instructions. PCR amplification was performed with 2.5 ng of cDNA sample.

2.4. Western blot analysis

The crude membrane fractions were prepared from MKN45 cells and Western blot analysis was performed as described previously [13,14]. As a positive control, brush border membrane fractions prepared from Caco-2 cells were used. Rabbit anti human PEPT1 antibody was raised and characterized as described [15].

2.5. Uptake study

The uptake of [^{3}H]glycylsarcosine ([^{3}H]Gly-Sar) and 2-deoxy-D-[^{3}H]glucose (2[^{3}H]DG) by MKN45 cells was examined according to our previous studies [16]. In the case of 2[^{3}H]DG uptake, uptake medium not containing D-glucose was used. MKN45 cells were seeded on 12-well plate at a cell density of 1×10^5 cells per well. The protein content of cell monolayers solubilized in 1 N NaOH was determined by the method of Bradford [17], using a Bio-Rad protein assay kit (Bio-Rad, Richmond, CA) with bovine γ-globulin as a standard.

2.6. 5-FU and CDDP treatment of MKN45 cells

At 3 days after seeding, MKN45 cells were exposed to 5-FU or CDDP at the concentrations and for the periods indicated in the figures. Both 5-FU and CDDP were dissolved with dimethylsulfoxide (DMSO). The final concentration of DMSO in the treatment medium was 0.1%. The treatment medium was exchanged every 24 h.

2.7. Statistical analysis

Results were expressed in the figures as the mean ± SE. Data were analyzed with a nonpaired *t*-test or a one-way analysis of variance followed by Scheffe's test.

3. Results

PEPT1 mRNA was detected in MKN45 cells by RT-PCR analysis (Fig. 1), and Western blot analysis also showed PEPT1 protein expression in MKN45 cells (Fig. 1). These findings suggested that PEPT1 was expressed in gastric cancer cells.

To confirm the functional properties of PEPT1 in MKN45 cells, we further assessed the transport

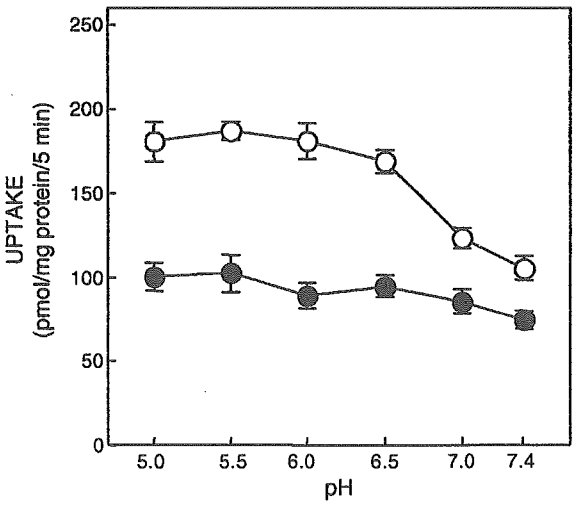

Fig. 2. Dependence on pH of [^{3}H]Gly-Sar uptake by MKN45 cells. The cells were incubated for 5 min at 37 °C at various pH with [^{3}H]Gly-Sar (50 μM) in the absence (○) or presence (●) of 5 mM glycylsarcosine in incubation medium. Each point represents the mean ± SE for three monolayers from a typical experiment.

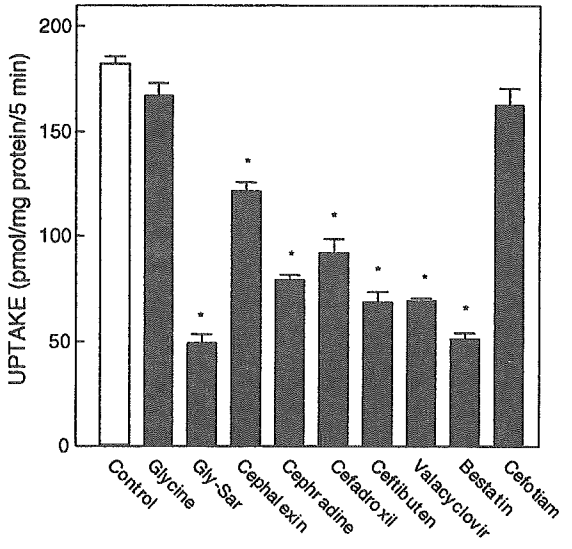

Fig. 3. Effects of various peptide-like drugs on [^{3}H]Gly-Sar uptake by MKN45 cells. The cells were incubated for 5 min at 37 °C with [^{3}H]Gly-Sar (50 μM) in the absence (□) or presence (■) of 10 mM of each drug in incubation medium (pH 6.0). Each column represents the mean±SE for three monolayers from a typical experiment. *$P<0.01$, significantly different from control.

characteristics of [^{3}H]Gly-Sar. [^{3}H]Gly-Sar uptake by MKN45 cells was maximal at around pH 5.5 (Fig. 2), and significantly inhibited in the presence of excess PEPT1 substrates such as cephradine and bestatin, but not by glycine and cefotiam, which were not transported by PEPT1 (Fig. 3). We then examined the concentration dependence of [^{3}H]Gly-Sar uptake by MKN45 cells. As shown in Fig. 4, Eadie–Hofstee plot analysis suggested that a single transporter was involved in MKN45 cells. The Michaelis–Menten constant (Km) value and the maximum uptake rates (V_{max}) were calculated to be 1.56±0.24 mM, and 4.17±0.19 nmol mg protein^{-1} min^{-1}, respectively, from three separate experiments. These characteristics of Gly-Sar transport are similar to those of transport by PEPT1 [1].

To examine whether the transport activity of PEPT1 was altered by anticancer drugs, we compared the uptake of [^{3}H]Gly-Sar and 2[^{3}H]DG, a substrate of GLUT1, after treatment with 5-FU and CDDP in MKN45 cells. [^{3}H]Gly-Sar transport was significantly increased by the treatment with 1 and 5 μg/mL of 5-FU for 72 h, but 2[^{3}H]DG transport was markedly decreased by 5-FU treatment in a concentration and time-dependent manner (Fig. 5). On the other hand, CDDP at 0.5–5 μg/mL did not alter the [^{3}H]Gly-Sar and 2[^{3}H]DG transport (Fig. 6). We then treated MKN45 cells with 5-FU alone (1 μg/mL), CDDP alone (1 μg/mL) and the two agents combined (5-FU, 1 μg/mL; CDDP, 1 μg/mL), because both drugs are simultaneously administered to patients with FP therapy in clinical situations. As shown in Fig. 7, the effect of simultaneous treatment of 5-FU and CDDP on PEPT1 and GLUT1 was similar to that of 5-FU treatment alone, suggesting no additive effect of the two drugs on PEPT1 activity.

Next, we examined the mRNA expression level on 5-FU treatment using the real-time PCR method. We treated MKN45 cells with 10 μg/mL of 5-FU for 72 h, because these conditions had the greatest effect on the cells as assessed in terms of cellular protein content (Fig. 8). As shown in Fig. 9, mRNA expression of GLUT1 and GAPDH in 5-FU treated cells were significantly reduced, but that of PEPT1 was slightly increased. We also found that PEPT1 protein was significantly increased by 5-FU treatment (Fig. 10). These results were consistent with the findings that

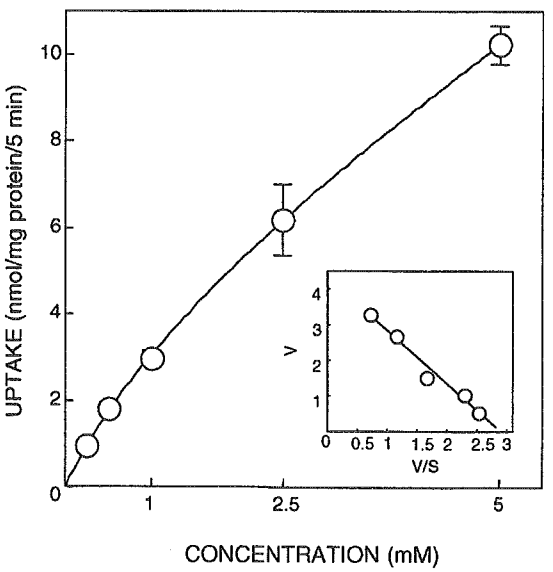

Fig. 4. Concentration-dependence of [^{3}H]Gly-Sar uptake by MKN45 cells. The cells were incubated for 5 min at 37 °C with various concentrations of [^{3}H]Gly-Sar in the incubation medium (pH 6.0). Each point represents the mean±SE for three monolayers from a typical experiment. Insets: Eadie-Hofstee plots of Gly-Sar uptake. V, uptake rate (nmol mg protein^{-1} 5 min^{-1}); S, Gly-Sar concentration (mM). Each point represents the mean±SE for three monolayers from a typical experiment.

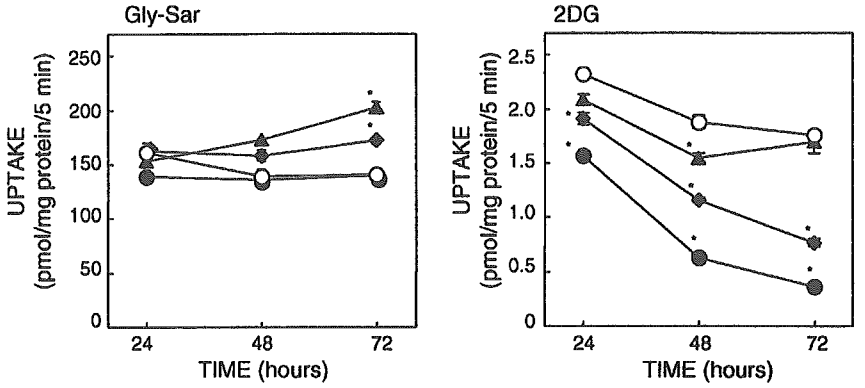

Fig. 5. Effect of 5-FU treatment on [^{3}H]Gly-Sar and 2[^{3}H]DG uptake by MKN45 cells. The cells were cultured with RPMI medium containing different concentrations of 5-FU (1 μg/mL (▲), 5 μg/mL (◆), and 10 μg/mL(●)), and 0.1% DMSO as a control (○). After 24–72 h treatment with 5-FU, uptake activity of PEPT1 and GLUT1 was examined with [^{3}H]Gly-Sar (50 μM) and 2[^{3}H]DG (71.4 nM), respectively. Each point represents the mean ± SE for three monolayers from a typical experiment. *$P<0.01$, significantly different from control in each period.

PEPT1 activity was maintained in spite of a decrease in cellular protein. It is, therefore, suggested that the level of PEPT1 protein per living cell increased during the treatment with 5-FU.

4. Discussion

In the present study, we have demonstrated that PEPT1 is functionally expressed in MKN45 cells. Because PEPT1 is not expressed in the normal stomach, the expression of PEPT1 in MKN45 cells may be induced by malignant transformation. PEPT1 was also expressed in pancreatic cancer cells such as AsPC-1 and Capan-2 [2] and the cholangiocarcinoma cell line SK-ChA-1 [3]. It is, therefore, speculated that high levels of PEPT1 may provide cancer cells with a metabolic advantage. Alterations of nutrient transporters in cancer cells have been used for diagnosis or treatment. For example, positron emission tomography (PET) using [^{18}F]-2-fluoro-2-deoxy-D-glucose (FDG) has been widely used in the non-invasive imaging of malignancies, based on the altered uptake of glucose mediated by overexpressed GLUT1 in cancer cells [18,19]. Furthermore, as a candidate for target

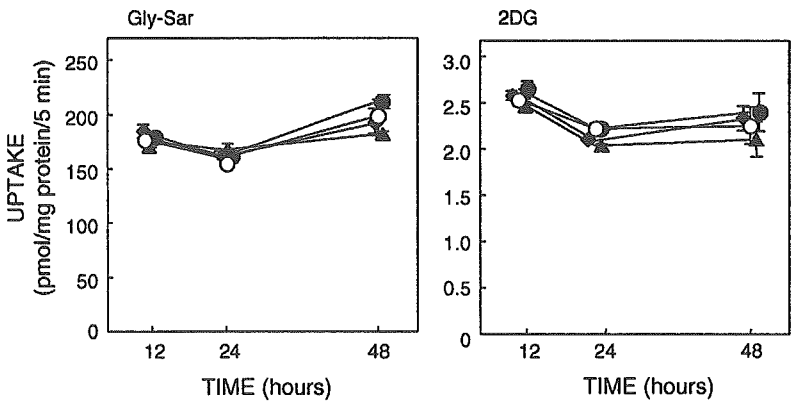

Fig. 6. Effect of CDDP treatment on [^{3}H]Gly-Sar and 2[^{3}H]DG uptake by MKN45 cells. The cells were incubated with RPMI medium containing different concentrations of CDDP (0.5 μg/mL (▲), 1 μg/mL (◆), and 5 μg/mL (●)), and 0.1% DMSO as a control (○). After 12–48 h treatment with CDDP, uptake activity of PEPT1 and GLUT1 was examined with [^{3}H]Gly-Sar (50 μM) and 2[^{3}H]DG (71.4 nM), respectively. Each point represents the mean ± SE for three monolayers from a typical experiment. *$P<0.01$, significantly different from control in each period.

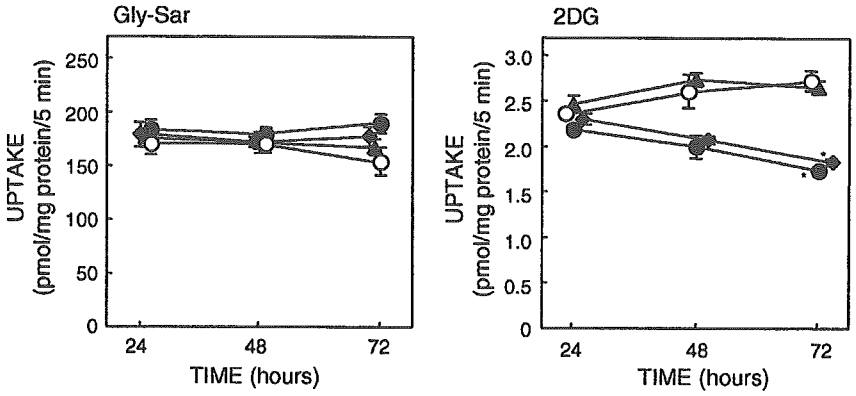

Fig. 7. Effect of simultaneous treatment with 5-FU and CDDP on [^{3}H]Gly-Sar and 2[^{3}H]DG uptake by MKN45 cells. The cells were incubated with RPMI medium containing 5-FU (1 μg/mL) (♦), CDDP (1 μg/mL) (▲), 5-FU (1 μg/mL) + CDDP (1 μg/mL) (●) and 0.1% DMSO as a control (○). After 24–72 h treatment, uptake activity of PEPT1 and GLUT1 was examined with [^{3}H]Gly-Sar (50 μM) and 2[^{3}H]DG (71.4 nM), respectively. Each point represents the mean ± SE for 12 monolayers from four separate experiments ([^{3}H]Gly-Sar) and three monolayers (2[^{3}H]DG). *$P<0.01$, significantly different from control in each period.

molecules for cancer therapy, transporter molecules have been widely investigated. For example, Noguchi et al. [20] demonstrated that the suppression of GLUT1 mRNA using an antisense method resulted in a decrease in tumor growth, and Fuchs et al. [21] reported that antisense RNA targeting an amino acid transporter (ATB^0/ASCT2) elicits apoptosis. As to PEPT1, the development of a drug delivery system targeting cancer cells has been attempted [4,5]. At present, it is not clear how PEPT1 is regulated in cancer cells, but the elucidation of signal pathways to induce the expression of PEPT1 may provide useful information on the cellular physiology of cancer cells and for the target strategy of anticancer drugs utilizing PEPT1.

5-FU is one of the most effective anticancer drugs and used in chemotherapy against a variety of solid tumors including gastric cancer [22]. It has been demonstrated that 5-FU altered the expression of various genes such as the p53 [23] and inducible nitric oxide synthase [24] in gastric cancer cells, and that these alterations may contribute to the pharmacological effects of 5-FU. Although 5-FU-based chemotherapy improves survival, drug resistance remains a significant limitation to the clinical use of 5-FU. The present study also showed that GLUT1 and GAPDH levels in MKN45 cells were significantly decreased by 5-FU treatment. In contrast, the function and expression of PEPT1 in living cells were enhanced by 5-FU treatment, suggesting that the supply of small peptides for MKN45 cells was maintained in spite of 5-FU-induced cell injury. Although the exact mechanisms responsible for the resistance of PEPT1 to

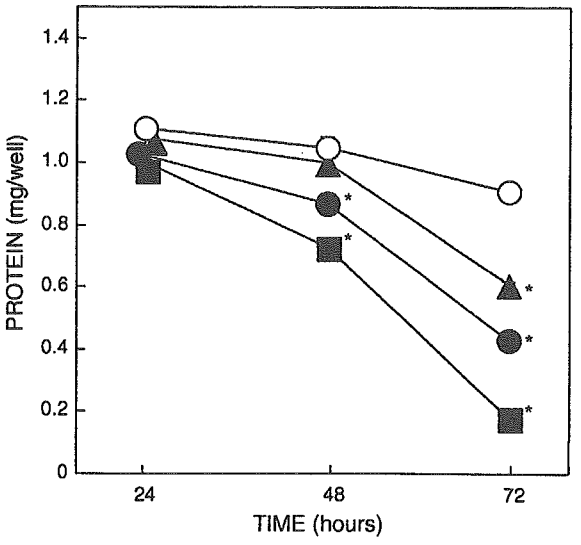

Fig. 8. Effect of 5-FU on cellular protein content in MKN45 cells. The cells were cultured with RPMI medium containing different concentrations of 5-FU (1 μg/mL (▲), 5 μg/mL (♦), and 10 μg/mL (●)), and 0.1% DMSO as a control (○). After 24–72 h treatment with 5-FU, the protein contents were measured. Each point represents the mean ± SE for three monolayers from a typical experiment. *$P<0.01$, significantly different from control in each period.

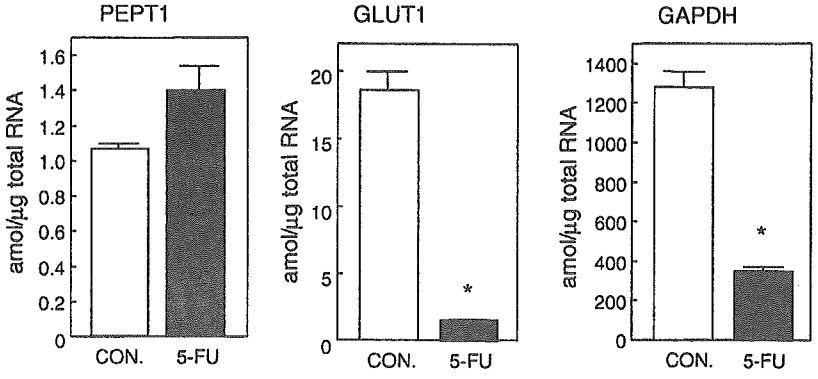

Fig. 9. Effects of 5-FU on the amount of PEPT1, GLUT1 and GAPDH mRNA expression by MKN45 cells. After the cells were cultured with RPMI medium containing 5-FU (10 μg/mL) for 72 h, total RNA was extracted and reverse-transcribed. For real-time PCR, 2.5 ng cDNA samples were analyzed with specific oligonucleotide primers and TaqMan probes. Each column represents the mean ± SE for three monolayers from a typical experiment. *$P < 0.01$, significantly different from control.

5-FU are unclear, the increased stability of PEPT1 mRNA and protein or some stress-induced factors may be involved. Similarly, it has been demonstrated that the function of PEPT1 was resistant to cell damage caused by starvation [25,26], and the administration of 5-fluorouracil (5-FU) [7], and cyclophosphamide [8]. These findings suggested that PEPT1 is resistant to severe stress. Because FDG uptake during PET increased depending on the expression of GLUT1, apparent anti-tumor effects of anticancer drugs such as 5-FU may be assessed based on decreased GLUT1 activity. But considering the clinical effects of 5-FU, an assessment of chemotherapy based only on GLUT1 may not be enough because a sustained supply of peptides and other nutrients results in cell survival. Some poorly differentiated colon and gastric cancer cell lines including MKN45 cells are reported to be survived in cultures not containing glucose and amino acids [27]. In this way, the resistance of tumor cells to glucose and amino acid deprivation may relate to the metabolism of other nutrients such as small peptides. Our study could suggest that ectopic PEPT1 activity and resistance to severe conditions in some gastric cancer cells enhances cell survival, and PEPT1 has the capacity to become a target molecule from the viewpoint of drug discovery and delivery.

In conclusion, our findings showed that PEPT1 is expressed and functioned in MKN45 cells. The function of PEPT1 was unaffected by the cellular injury induced by 5-FU treatment. Further studies concerning the pathophysiological role of PEPT1 in cancer cells and regulatory mechanisms of PEPT1 should facilitate the development of effective chemotherapeutics.

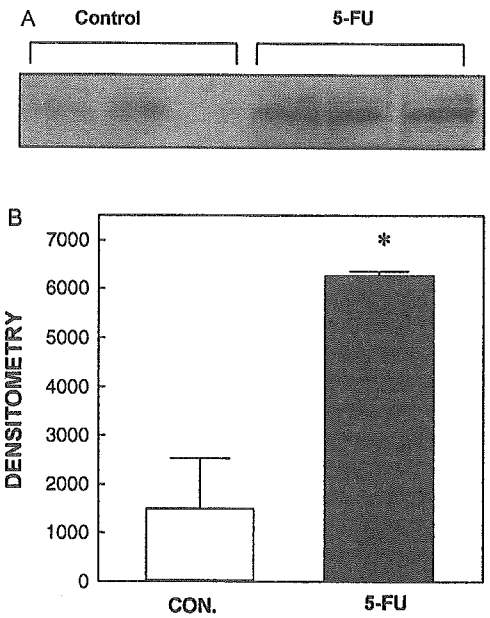

Fig. 10. Effect of 5-FU on the amount of PEPT1 protein expression by MKN45 cells. (A) After the cells were cultured with RPMI medium containing 5-FU (10 μg/mL) for 72 h, crude membrane was prepared, and PEPT1 protein expression was detected by Western blotting using PEPT1-specific antibody. Cell lysates, 50 μg each, were loaded into each lane. (B) PEPT1 protein levels were quantified by scanning densitometry. Each column represents the mean ± SE of three monolayers from a typical experiment. *$P < 0.01$, significantly different from control.

Acknowledgements

This work was supported in part by a Grant-in-Aid for Scientific Research from the Ministry of Education, Culture, Sports, Science and Technology of Japan.

References

[1] T. Terada, K. Inui, Peptide transporters: structure, function, regulation and application for drug delivery, Curr. Drug Metab. 5 (2004) 85–94.

[2] D.E. Gonzalez, K.M. Covitz, W. Sadee, R.J. Mrsny, An oligopeptide transporter is expressed at high levels in the pancreatic carcinoma cell lines AsPc-1 and Capan-2, Cancer Res. 58 (1998) 519–525.

[3] I. Knutter, I. Rubio-Aliaga, M. Boll, G. Hause, H. Daniel, K. Neubert, M. Brandsch, H^+-peptide cotransport in the human bile duct epithelium cell line SK-ChA-1, Am. J. Physiol. Gastrointest. Liver Physiol. 283 (2002) G222–G229.

[4] T. Nakanishi, I. Tamai, A. Takaki, A. Tsuji, Cancer cell-targeted drug delivery utilizing oligopeptide transport activity, Int. J. Cancer 88 (2000) 274–280.

[5] J. Neumann, M. Brandsch, δ-aminolevulinic acid transport in cancer cells of the human extrahepatic biliary duct, J. Pharmacol. Exp. Ther. 305 (2003) 219–224.

[6] S.A. Adibi, Regulation of expression of the intestinal oligopeptide transporter (Pept-1) in health and disease, Am. J. Physiol. Gastrointest. Liver Physiol. 285 (2003) G779–G788.

[7] H. Tanaka, K.I. Miyamoto, K. Morita, H. Haga, H. Segawa, T. Shiraga, et al., Regulation of the PepT1 peptide transporter in the rat small intestine in response to 5-fluorouracil-induced injury, Gastroenterology 114 (1998) 714–723.

[8] J. Satoh, T. Tsujikawa, Y. Fujiyama, T. Bamba, Nutritional benefits of enteral alanyl-glutamine supplementation on rat small intestinal damage induced by cyclophosphamide, J. Gastroenterol. Hepatol. 18 (2003) 719–725.

[9] F. Berlioz, J.J. Maoret, H. Paris, M. Laburthe, R. Farinotti, C. Roze, α_2-adrenergic receptors stimulate oligopeptide transport in a human intestinal cell line, J. Pharmacol. Exp. Ther. 294 (2000) 466–472.

[10] T. Fujita, Y. Majikawa, S. Umehisa, N. Okada, A. Yamamoto, V. Ganapathy, F.H. Leibach, σ Receptor ligand-induced up-regulation of the H^+/peptide transporter PEPT1 in the human intestinal cell line Caco-2, Biochem. Biophys. Res. Commun. 261 (1999) 242–246.

[11] K.F. Becker, G. Keller, H. Hoefler, The use of molecular biology in diagnosis and prognosis of gastric cancer, Surg. Oncol. 9 (2000) 5–11.

[12] W. Yasui, N. Oue, R. Ito, K. Kuraoka, H. Nakayama, Search for new biomarkers of gastric cancer through serial analysis of gene expression and its clinical implications, Cancer Sci. 95 (2004) 385–392.

[13] H. Saito, M. Okuda, T. Terada, S. Sasaki, K. Inui, Cloning and characterization of a rat H^+/peptide cotransporter mediating absorption of β-lactam antibiotics in the intestine and kidney, J. Pharmacol. Exp. Ther. 275 (1995) 1631–1637.

[14] T. Terada, H. Saito, M. Mukai, K. Inui, Identification of the histidine residues involved in substrate recognition by a rat H^+/peptide cotransporter, PEPT1, FEBS Lett. 394 (1996) 196–200.

[15] K. Ashida, T. Katsura, H. Motohashi, H. Saito, K. Inui, Thyroid hormone regulates the activity and expression of the peptide transporter PEPT1 in Caco-2 cells, Am. J. Physiol. Gastrointest. Liver Physiol. 282 (2002) G617–G623.

[16] T. Terada, K. Sawada, H. Saito, Y. Hashimoto, K. Inui, Functional characteristics of basolateral peptide transporter in the human intestinal cell line Caco-2, Am. J. Physiol. 276 (1999) G1435–G1441.

[17] M.M. Bradford, A rapid and sensitive method for the quantitation of microgram quantities of protein utilizing the principle of protein-dye binding, Anal. Biochem. 72 (1976) 248–254.

[18] T. Kurokawa, Y. Yoshida, K. Kawahara, T. Tsuchida, H. Okazawa, Y. Fujibayashi, et al., Expression of GLUT-1 glucose transfer, cellular proliferation activity and grade of tumor correlate with [F-18]-fluorodeoxyglucose uptake by positron emission tomography in epithelial tumors of the ovary, Int. J. Cancer 109 (2004) 926–932.

[19] M. Kunkel, T.E. Reichert, P. Benz, H.A. Lehr, J.H. Jeong, S. Wieand, et al., Overexpression of Glut-1 and increased glucose metabolism in tumors are associated with a poor prognosis in patients with oral squamous cell carcinoma, Cancer 97 (2003) 1015–1024.

[20] Y. Noguchi, A. Saito, Y. Miyagi, S. Yamanaka, D. Marat, C. Doi, et al., Suppression of facilitative glucose transporter 1 mRNA can suppress tumor growth, Cancer Lett. 154 (2002) 175–182.

[21] B.C. Fuchs, J.C. Perez, J.E. Suetterlin, S.B. Chaudhry, B.P. Bode, Inducible antisense RNA targeting amino acid transporter ATB^0/ASCT2 elicits apoptosis in human hepatoma cells, Am. J. Physiol. Gastrointest. Liver Physiol. 286 (2004) G467–G478.

[22] D.B. Longley, D.P. Harkin, P.G. Johnston, 5-fluorouracil: mechanisms of action and clinical strategies, Nat. Rev. Cancer 3 (2003) 330–338.

[23] M. Osaki, S. Tatebe, A. Goto, H. Hayashi, M. Oshimura, H. Ito, 5-Fluorouracil (5-FU) induced apoptosis in gastric cancer cell lines: role of the p53 gene, Apoptosis 2 (1997) 221–226.

[24] I.D. Jung, S.Y. Yang, C.G. Park, K.B. Lee, J.S. Kim, S.Y. Lee, et al., 5-Fluorouracil inhibits nitric oxide production through the inactivation of IκB kinase in stomach cancer cells, Biochem. Pharmacol. 64 (2002) 1439–1445.

[25] X. Pan, T. Terada, M. Okuda, K. Inui, Altered diurnal rhythm of intestinal peptide transporter by fasting and its effects on the pharmacokinetics of ceftibuten, J. Pharmacol. Exp. Ther. 307 (2003) 626–632.
[26] H. Ogihara, T. Suzuki, Y. Nagamachi, K. Inui, K. Takata, Peptide transporter in the rat small intestine: ultrastructural localization and the effect of starvation and administration of amino acids, Histochem. J. 31 (1999) 169–174.
[27] K. Izuishi, K. Kato, T. Ogura, T. Kinoshita, H. Esumi, Remarkable tolerance of tumor cells to nutrient deprivation: possible new biochemical target for cancer therapy, Cancer Res. 60 (2000) 6201–6207.

Available online at www.sciencedirect.com
SCIENCE DIRECT
Biochemical Pharmacology 70 (2005) 1756–1763
Biochemical Pharmacology
www.elsevier.com/locate/biochempharm

Expression profiles of various transporters for oligopeptides, amino acids and organic ions along the human digestive tract

Tomohiro Terada [a], Yutaka Shimada [b], Xiaoyue Pan [a], Koshiro Kishimoto [a], Takaki Sakurai [c], Ryuichiro Doi [b], Hisashi Onodera [b], Toshiya Katsura [a], Masayuki Imamura [b], Ken-ichi Inui [a,*]

[a] *Department of Pharmacy, Kyoto University Hospital, Sakyo-ku, Kyoto 606-8507, Japan*
[b] *Surgery and Surgical Basic Science, Graduate School of Medicine, Kyoto University, Japan*
[c] *Laboratory of Anatomic Pathology, Kyoto University Hospital, Japan*

Received 31 August 2005; accepted 28 September 2005

Abstract

Various transporters such as H^+/peptide cotransporter PEPT1 are expressed in the intestine, and play important physiological and pharmacological roles in the body. Present study was performed to examine the expression profile of 20 kinds of transporters (PEPT1 and 2, P-glycoprotein, amino acid transporters and organic ion transporters) along the human digestive tract, especially focusing on PEPT1. Using normal mucosal specimens, real-time polymerase chain reactions were carried out. Immunoblot analyses were also performed for PEPT1 expression. PEPT1 mRNA was highly expressed in the small intestine (duodenum > jejunum > ileum) compared to other tissues, and some patients showed a significant level of expression in the stomach. The expressional pattern of PEPT1 in the stomach and histological diagnosis indicated that gastric PEPT1 originated from the intestinal metaplasia. The amino acid transporters showed unique mRNA expression levels and distributions in the digestive tract. For example, the expression levels of B^0AT1, a Na^+-dependent and chloride-independent neutral amino acid transporter, were increased from the duodenum to ileum, which pattern is completely inverted to that for PEPT1. There is little expression of organic ion transporters except for organic cation/carnitine transporter OCTN2. In conclusion, PEPT1 was abundantly expressed in the small intestine, and the reciprocal expression of PEPT1 and B^0AT1 may serve for the efficient absorption of protein digestive products.

Keywords: Protein absorption; Digestive tract; Transporter; PEPT1; B^0AT1; OCTN2; Organic ion transporter

1. Introduction

Cellular uptake of small peptides (di- and tri-peptides) is mediated by a H^+/peptide cotransporter at the brush-border membranes of intestinal absorptive epithelial cells [1,2]. Cloning studies have clarified the molecular nature of the intestinal H^+/peptide cotransporter (PEPT1) in various species [2,3]. Another H^+/peptide cotransporter, human PEPT2 is expressed mainly in the kidney, but not in the small intestine, and has a higher affinity for most substrates [3]. As PEPT1 has broad substrate specificity, the intestinal absorption of several pharmacologically active drugs, such as oral β-lactam antibiotics and the anti-viral agent valacyclovir are mediated by this transporter, and therefore, PEPT1 also plays important roles as a drug transporter [3].

In addition to PEPT1, various amino acid transport systems, such as L, y^+, y^+L, $b^{0,+}$, A, ASC, B^0, $B^{0,+}$ and X_{AG}^- are expressed in the small intestinal epithelial cells. These systems have been classified by their ion-dependence and substrate specificity [4], and the molecular nature of each system has been identified [5,6]. For example, system B^0, which is a Na^+-dependent and chloride-independent transporter, is responsible for the uptake of most neutral amino acids at the brush-border membranes of intestinal epithelial cells [7,8]. Two independent groups have recently isolated and characterized the transporter cDNA corresponding to system B^0 (B^0AT1), and demonstrated that a mutation of B^0AT1 results in the Hartnup disorder [9,10].

* Corresponding author. Tel.: +81 75 751 3577; fax: +81 75 751 4207.
E-mail address: inui@kuhp.kyoto-u.ac.jp (K.-i. Inui).

0006-2952/$ – see front matter © 2005 Elsevier Inc. All rights reserved.
doi:10.1016/j.bcp.2005.09.027

Although the number of peptide transporters is smaller than that of amino acid transporters, numerous investigations have shown that the peptide transporters play a major role in the completion of the final step of protein digestion in the human intestine [1]. These findings led us to examine the expression levels of each transporter along the human digestive tract. Thus, in the present study, using normal portions of mucosal samples from cancer patients treated surgically, mRNA expression levels of PEPT1 and seven amino acid transporters were qualified by real-time PCR techniques. Furthermore, to investigate the pharmacokinetic aspects of PEPT1, we compared mRNA expression level of PEPT1 with those of other drug transporters, i.e., organic ion transporters. We previously examined the expression profiles of organic ion transporters in the kidney [11], but there is little information about their expression in the human gut.

2. Material and methods

2.1. Patients and tissue sampling

The mucosal samples from normal tissues along the digestive tract and normal pancreatic tissue were obtained from cancer patients during surgery at the First Department of Surgery, Kyoto University Hospital. Normal mucosal samples were resected at the site most distant from the affected portions. Table 1 shows the number, sex and age of patients for each tissue sample. No patients underwent preoperative chemotherapy and/or radiation therapy. The samples were frozen in liquid nitrogen and stored at −80 °C until RNA extraction and membrane preparation. This study was conducted in accordance with the Declaration of Helsinki and its amendments, and was approved by the Ethics Committee of Kyoto University (G-39). Written informed consent was obtained from all patients for surgery and use of their resected samples.

2.2. Isolation of total RNA

Total cellular RNA was isolated from the tissue samples using a MagNA Pure LC RNA isolation Kit II (Roche Diagnostic GmbH, Mannheim, Germany) according to the manufacturer's instructions, and the concentrations of total cellular RNA were measured by spectrophotometry. Isolated total RNA was reverse-transcribed and the reaction mixtures were used for real-time PCR.

Table 1
The number, sex and age of patients for each tissue sample

	n	Male	Female	Age (years)
Esophagus	16	13	3	59.3 ± 1.6
Stomach	31	20	11	64.4 ± 2.3
Duodenum	13	7	6	63.8 ± 2.2
Jejunum	15	13	2	66.6 ± 3.7
Ileum	10	4	6	65.3 ± 5.7
Colon	15	8	7	71.6 ± 3.1
Rectum	15	11	4	64.6 ± 3.0
Pancreas	9	3	6	61.8 ± 2.8

2.3. Real-time PCR

Primers and probes for PEPT1 and 2, seven amino acid transporters and urate transproter (URAT1) were designed using the Primer Express® software program (Table 2). Those for multidrug resistance 1 (MDR1) [12] and organic ion transporters [11] were previously designed. Oligonucleotide probes were labelled with a fluorogenic dye, 6 carboxyfluorescein (Fam) and quenched with 6 carboxy-tetramethylrhodamine (Tamra) (Table 2). Real-time PCR was performed in an ABI PRISM 7700 (Applied Biosystems, Foster, CA) and quantification by use of standard plasmid DNA was performed as described previously [11]. For each reaction, the assay was carried out in duplicate. Glyceroladehyde 3-phosphate denydrogenase (GAPDH) mRNA was also measured as an internal control with GAPDH control reagent (Applied Biosystems).

2.4. Antibodies

Rabbit anti-human PEPT1 antibody was prepared previously, and the specificity was already confirmed [13]. Mouse anti-Na^+/K^+-ATPase monoclonal antibody was purchased from Upstate Biotechnology (Lake Placid, NY). For immunohistochemistry, we used anti-CD10 antibody (Novocastra Laboratories Ltd., Newcastle upon Tyne, UK).

2.5. Western blot analysis

Crude plasma membranes were prepared from tissue samples taken along the digestive tract as described previously [11]. Western blot analyses using affinity-purified anti-PEPT1 antibody [13] and mouse monoclonal Na^+/K^+-ATPase antibody [11] were carried out based on our previous reports.

2.6. Immunohistochemistry

Paraffin-embeded sections were stained for CD10 antibody. The sections were deparaffinized, and antigens were retrieved by autoclave in 10 mM EDTA buffer (pH 8.0) for 15 min. Non-specific antigen was blocked by 10% normal horse serum for 30 min at room temperature. Anti-CD10 antibody (×50) in PBS containing 1% bovine serum albumin was applied and sections were incubated at 37 °C for 32 min. Slides were washed six times in PBS, and then incubated with biotinylated horse anti-mouse antibody for 40 min at room temperature. The slides were then counterstained with hematoxylin.

Table 2
Primer sets and probes used for real-time PCR

	Sequence	Nucleotide numbers	Accession number
PEPT1			NM_005073
Forward primer	attgtgtcgctctccattgtctac	306–329	
Reverse primer	atgacctcacagaccacaaccat	389–367	
TaqMan probe	ttggacaagcagtcacctcagtaagctcca	334–363	
PEPT2			NM_021082
Forward primer	ttaaacaaggccccagagactct	2382–2404	
Reverse primer	cccacttagttctggacctgctt	2463–2445	
TaqMan probe	tgccccaaccagtcttcaggaggaag	2410–2439	
B^0AT1			XM_291120
Forward primer	gtgtggacaggttcaataaggacat	1646–1670	
Reverse primer	ccacgtgacttgccagaagat	1719–1699	
TaqMan probe	tcatgatcggccacaagcccaa	1676–1697	
ASCT2			U53347
Forward primer	gcgagaaatatcttcccttcca	1152–1202	
Reverse primer	gttccggtgatattcctctcttca	1266–1243	
TaqMan probe	tgtcagcagcctttcgctcatactctacca	1209–1238	
$b^{0,+}AT$			AF141289
Forward primer	ggcctgacgattctaggactca	1344–1365	
Reverse primer	ggagccagaaccaaaaacaca	1468–1448	
TaqMan probe	atcaaggtgcccgtagtcattcccgt	1404–1429	
LAT1			AF104032
Forward primer	ggaagacacccgtggagtgt	1421–1440	
Reverse primer	acaggacggtcgtggagaag	1552–1533	
TaqMan probe	tggaaaaacaagcccaagtggctcc	1498–1522	
LAT2			AF171669
Forward primer	tgaggagcttgttgatccctaca	988–1010	
Reverse primer	gcgacattggcaaagacataca	1080–1059	
TaqMan probe	tcccagagccatcttcatctccatcc	1018–1043	
y^+LAT1			AF092032
Forward primer	gatccatgttgagcggttcac	1336–1356	
Reverse primer	ccacgcacaagtagatcaatgc	1412–1391	
TaqMan probe	ccagtgccttctctgctcttcaatggtatc	1358–1387	
ATA2			AF259799
Forward primer	gacagcagcagctacagttcca	66–87	
Reverse primer	cataatggcttttcagagcagctt	144–121	
TaqMan probe	agcgacttcaactactcctaccccaccaag	90–119	
URAT1			AB071863
Forward primer	agctcttggaccccaatgc	437–455	
Reverse primer	cttcagagcgtgagagtcacaca	560–582	
TaqMan probe	cgcagcatcttcacctccacaatcgt	517–542	

Primers and probes used for real-time PCR. All primers and probes were designed using Primer Express software from Applied Biosystems. Primers were tested using RT-PCR and only those yielding a single band of the expected size were used for subsequent real-time PCR experiments.

3. Results

3.1. Quantification of PEPT1 and PEPT2 mRNA in tissues along the digestive tract and pancreas

First, to verify the conditions and experimental techniques, MDR1 mRNA expression levels were measured (Fig. 1 right). We previously found that the level of MDR1 mRNA in the jejunum from living-donor liver transplantation patients was 0.41 ± 1.19 amol/μg of total RNA (mean ± S.E., $n = 48$) using a competitive PCR-based method, and that the level of MDR1 mRNA correlated well with protein level [14]. In the present study, the MDR1 mRNA level in the jejunum was 2.73 ± 0.51 amol/μg of total RNA (mean ± S.E., $n = 16$). This value was similar to previously reported ones [14]. Furthermore, MDR1 mRNA levels gradually increased from the duodenum to ileum, well consistent with previous findings on the distribution of MDR1 mRNA [15] and P-glycoprotein [16] in the human small intestine (Fig. 1 right). The expression of MDR1 mRNA in the colon and rectum (Fig. 1 right) also corresponded to a previous report [17]. All these findings suggested that the conditions and experimental techniques were reliable.

We then examined the mRNA expression of PEPT1 and PEPT2 along the digestive tract (esophagus, stomach,

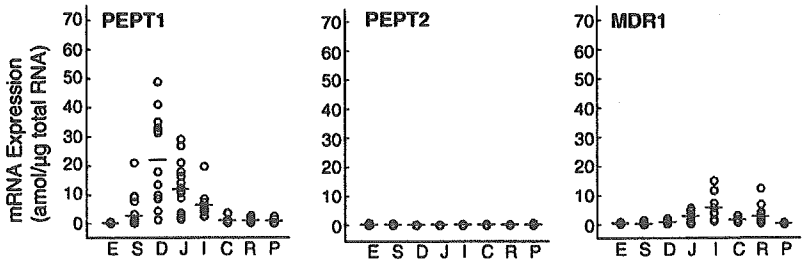

Fig. 1. mRNA expression of PEPT1, PEPT2 and MDR1 along the digestive tract (esophagus (E), stomach (S), duodenum (D), jejunum (J), ileum (I), colon (C), rectum (R)) and pancreas (P). Total cellular RNA was extracted from each tissue sample, and reverse-transcribed. The mRNA levels were determined by real-time PCR using an ABI prism 7700 sequence detector.

duodenum, jejunum, ileum, colon and rectum) and pancreas. As shown in Fig. 1 left, PEPT1 mRNA is highly expressed in the small intestine (duodenum > jejunum > ileum), but is not expressed or only slightly expressed in the esophagus, colon, rectum and pancreas. In the stomach, some patients showed a high level of PEPT1 mRNA. The tissue which showed the highest expression level was the duodenum (22.0 ± 4.23 amol/μg RNA). In contrast to PEPT1 mRNA, PEPT2 mRNA was not expressed in all tissues examined (Fig. 1 middle).

3.2. Western blot analysis

Fig. 2 shows Western blot analyses using crude membranes from each tissue. A primary band of about 80 kDa of PEPT1 protein was detected in the stomach, duodenum, jejunum and ileum, as observed in the mRNA analyses. In other tissues, no PEPT1 protein was detected. In the case of PEPT2 protein, there were no detectable bands in the tissue samples from along the digestive tracts (data not shown). The protein band of Na^+/K^+-ATPase was detected in all specimens (Fig. 2).

3.3. PEPT1 in the stomach

There is no expression of PEPT1 protein in the rat stomach [18]. On the other hand, the present study has demonstrated that some patients had a relatively high level of PEPT1 in the stomach, although there were interindividual differences. To clarify the distribution of PEPT1 in the gastric mucosa, fundus (the upper-third: U), body (the middle-third: M) and antrum (the lower-third: L) mucosa were assessed for PEPT1 protein expression when sections were available from one patient. As shown in Fig. 3,

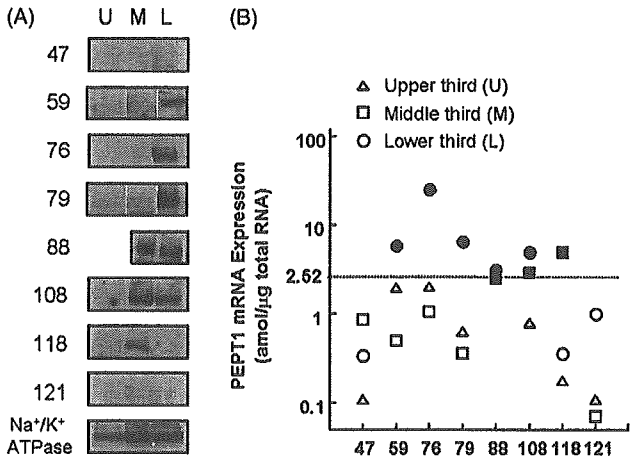

Fig. 3. PEPT1 expression in the gastric mucosa. (A) Crude membranes were isolated from the upper-third (U), middle-third (M) and lower-third (L) of the gastric mucosa from eight patients and subjected to Western blot analyses (50 μg protein/lane) for PEPT1 and Na^+/K^+-ATPase. Conditions for Western blotting were identical to those in Fig. 2. For Na^+/K^+-ATPase, representative data are shown. A sample for the upper-third of patient 88 was not obtained. (B) Relationship between mRNA and protein expression levels of PEPT1 in gastric mucosa. Closed symbols represent the samples with PEPT1 protein expression. When the mRNA level was more than 2.52 amol/μg of total RNA, the band for PEPT1 protein was detected.

PEPT1 protein was expressed in the antral mucosa in most cases, and well correlated with mRNA expression level. When the mRNA level was more than 2.52 amol/μg of total RNA, the band for PEPT1 protein was detected.

These expressional patterns and the histological diagnosis suggested that intestinal metaplasia may induce the expression of PEPT1 in the stomach. Intestinal metaplasia primarily affects the antrum in a patchy fashion, and the superficial gastric epithelium is replaced by intestinal goblet and absorptive cells [19]. Using paraffin sections

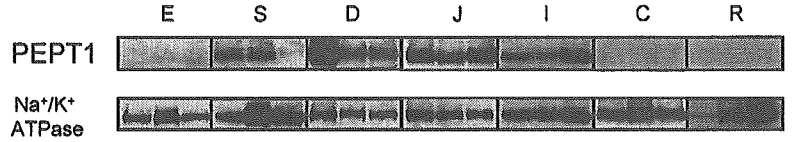

Fig. 2. Western blot analyses of crude membranes isolated from human tissues along the digestive tract for PEPT1 and Na^+/K^+ ATPase. Crude membranes were isolated from each tissue and subjected to Western blotting (50 μg protein/lane). Abbreviations for each tissue are identical to those in Fig. 1. PEPT1 protein was identified using affinity-purified anti-PEPT1 antibody (1:500 dilution). After the membranes were deprobed, Na^+/K^+-ATPase protein was detected by the mouse monoclonal anti Na^+/K^+-ATPase antibody (1:10,000).

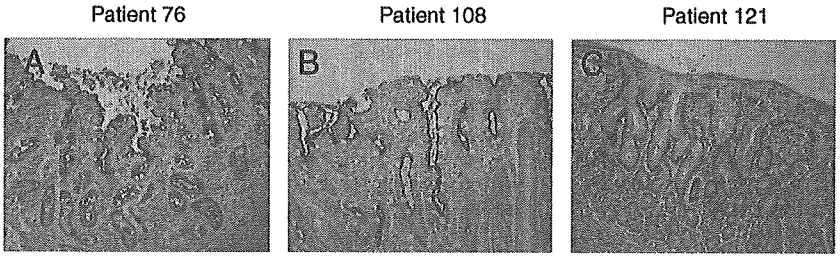

Fig. 4. Localization of CD10 in the intestinal metaplasia. (A and B) CD10 can be seen along the brush-border membranes of the luminal surface of the epithelium in antral mucosa from patients 76 and 108 (original magnification ×50). (C) Hematoxilin–eosin staining of antral mucosa from patient 121.

of antral mucosa from patients 76, 108 and 121, immunostaining for CD10 was carried out. CD10, also known as enkephalinase, has been shown to localize to the brush-border membranes of absorptive small intestinal enterocytes [20]. CD10 was positively expressed along the luminal surface of the epithelium of patients 76 and 108 (Fig. 4A and B), but not patient 121 (data not shown). Hematoxilin–eosin staining revealed that intestinal metaplasia did not occurr in patient 121 (Fig. 4C).

3.4. Comparison of mRNA expression levels of PEPT1 with those of amino acid transporters in the digestive tract

We next examined the expression profile of amino acid transporters in the digestive tract to compare with PEPT1. The human amino acid transporters examined here were mainly neutral amino acid transporters and reported to be important for intestinal epithelial transport, i.e., system B^0 (B^0AT1) [9,10], system ASC (ASCT2) [21], system $b^{0,+}$ ($b^{0,+}AT$) [22], system L (LAT1 [23,24] and LAT2 [25–27]), system y^+L, (y^+LAT1) [28] and system A (ATA2) [29]. It has been demonstrated that B^0AT1, ASCT2 and $b^{0,+}AT$ localized at the brush-border membranes of epithelial cells, whereas LAT1, LAT2, y^+LAT1 and ATA2 localized at the basolateral membranes.

Fig. 5 shows the mRNA expression levels along the digestive tract for the amino acid transporters localized to brush-border membranes: B^0AT1, ASCT2 and $b^{0,+}AT$. These three transporters exhibited distinguishable expression patterns. B^0AT1 mRNA levels were increased from duodenum to ileum like MDR1 mRNA levels. ASCT2 showed little expression in the small intestine, but significant expression in the large intestine (colon and rectum). In contrast, $b^{0,+}AT$ exhibited little expression in the digestive tract except for the stomach.

Fig. 6 shows the mRNA expression levels along the digestive tract for the amino acid transporters localized to basolateral membranes: LAT1, LAT2, y^+LAT1 and ATA2. ATA2 showed a strong expression in the tissues tested. LAT1 was preferentially expressed in the esophagus, stomach and pancreas, as compared with the small and large intestine. The expression of LAT2 was abundant in the stomach and rectum, and modest in the small intestine

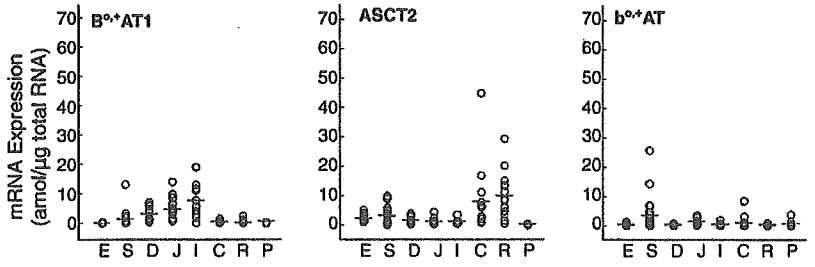

Fig. 5. mRNA expression of brush-border membrane-localized amino acid transporters B^0AT1, ASCT2 and $b^{0,+}AT$ along the digestive tract and pancreas. Abbreviations for each tissue and experimental methods are identical to those in Fig. 1.

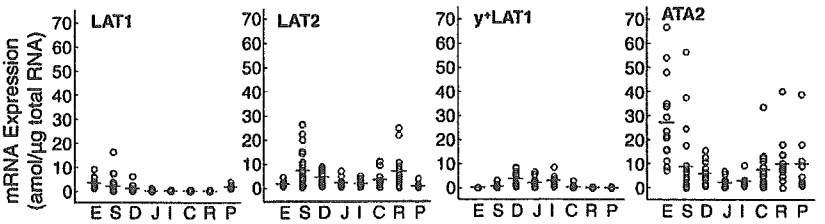

Fig. 6. mRNA expression of basolateral membrane-localized amino acid transporters LAT1, LAT2, y^+LAT1 and ATA2 along the digestive tract and pancreas. Abbreviations for each tissue and experimental methods are identical to those in Fig. 1.

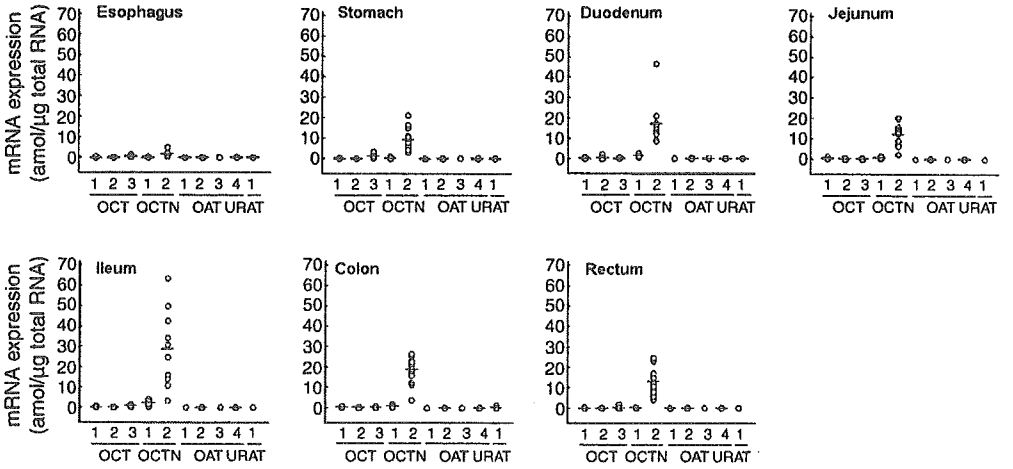

Fig. 7. mRNA expression of organic ion transporters along the digestive tract. Tested transporters are as follows: OCT1–3, OCTN1 and 2, OAT1–4 and URAT1. Experimental methods are identical to those in Fig. 1.

(duodenum, jejunum and ileum). In contrast, y^+LAT1 was predominantly expressed in the small intestine (duodenum, jejunum and ileum) with little expression in other tissues.

PEPT1 also works as a drug transporter. To compare the mRNA expression level of PEPT1 with other drug transporters, we selected organic ion transporter family including organic cation transporters (OCT1–3), organic cation/carnitine transporters (OCTN1 and 2), organic anion transporters (OAT1–4) and urate transporter (URAT1). These transporters are mainly expressed in the kidney [11] and play important roles for renal secretion of ionic drugs [30], but some transporters were suggested to mediate the intestinal secretion of drugs [31]. As shown in Fig. 7, there was little expression for organic ion transporters except for OCTN2. OCTN2 exhibited a similar expression level of PEPT1 in the intestine. In addition to intestine, OCTN2 exhibited abundant expression in the stomach, colon and rectum.

4. Discussion

In the present study, we have demonstrated that the mRNA expression level of PEPT1 is higher in the duodenum and jejunum than that of B^0AT1, ASCT2 and $b^{0,+}$AT, which are localized at the brush-border membranes, and is equal to that of B^0AT1 in the ileum. Previous works showed that luminal contents after protein ingestion mostly consist of two to six amino acids [32], and that most of the dipeptidase activity is located in the cytoplasm of mucosal cells [33]. Thus, higher expression levels of PEPT1 than amino acid transporters at brush-border membranes should support the nutritional importance of the intestinal absorption of small peptides for protein nutrition. The high expression levels of intestinal PEPT1 also emphasize the pharmacological implication of peptide transporters. The peptide-like drugs transported by PEPT1 showed good oral bioavailability [3]. Transport abilities of PEPT1, with great flexibility for structural modification, and high expression of PEPT1 in the small intestine should be helpful for drug development to improve the intestinal absorption of poorly absorbed drugs.

The expression level of PEPT1 mRNA showed a peak in the duodenum, and gradually decreased to the ileum. Interestingly, the expression gradient of B^0AT1 mRNA is completely inversed to that of PEPT1. These reciprocal axial gradients in the mRNA expression of PEPT1 and B^0AT1 well correspond to the transport activities of small peptides [34,35] and amino acids for system B [36], and may have physiological relevance and importance to the maintenance of optimal protein nutrition [37]. Namely, the ingested proteins are digested by the membrane-bound peptidases to generate a major portion of the absorbable products, namely, amino acids and small peptides. Though these peptidases are present throughout the small intestine, levels of activity are much higher in the ileum than in the jejunum [38], indicating that the concentrations of free amino acids in the lumen are gradually increased, while the luminal concentration of small peptides are gradually decreased as the luminal contents move along the intestine. Furthermore, K_m values of typical substrates for PEPT1 (glycylsarcosine) [39] and B^0AT1 (leucine) [10] were about 1 mM, suggesting that both transporters have similar kinetic parameters. It is, therefore, suggested that the efficient absorption of digestive products of proteins may be achieved by a good correlation between the expression profiles for PEPT1 and B^0AT1 and the luminal concentrations of the corresponding substrates along the intestine.

Using tissue biopsy samples, Gutmann et al. [40] demonstrated that the mRNA expression of human breast cancer resistance protein (BCRP) was maximal in the duodenum and decreased continuously down to the rectum [40]. This expression profile is contrast to that of MDR1 mRNA expression (Fig. 1 right), suggesting that BCRP and

MDR1 also complement the transport function each other along the digestive tract as the substrate specificity of both transporters is partially overlapping [41]. Taken together, reciprocal expression of functionally related membrane transporters along the digestive tract should be responsible for the efficient biological systems in physiology and pharmacology.

Recently, Dave et al. [42] examined the expression of heteromeric amino acid transporters along the murine intestine. Their major findings related to our study were as follows: (i) the main sites of mRNA expression of absorptive amino acid transporters ($b^{0,+}$AT, LAT2 and y^+LAT1) were the jejunum and ileum; (ii) a substantial level of LAT2 mRNA was found in the stomach, an organ not previously recognized as a major site of amino acid absorption and (iii) LAT1 was most abundant in brain and weakly expressed in the intestine except for the stomach. Most of these findings were also confirmed in the human intestine, although the expression levels of $b^{0,+}$AT, LAT2 and y^+LAT1were not so high in the human intestine as compared to mouse intestine. Mutations in $b^{0,+}$AT lead to the hereditary disease cystinuria [22], and characterized by renal loss and altered intestinal absorption of cationic amino acids and cystine. Interestingly, patients with cystinuria do not exhibit obvious symptoms of protein malabsorption because the affected amino acids are absorbed adequately in the form of small peptides [43]. The much higher levels of PEPT1 than $b^{0,+}$AT explain this compensation.

In the present study, PEPT1 was found to be expressed in the stomach, induced by intestinal metaplasia. Intestinal metaplasia is characterized by the transdifferentiation of gastric epithelial cells to an intestinal phenotype [19]. Several intestinal-specific gene products such as trefoil peptides [44] were reported to be expressed in the stomach after intestinal metaplasia. *CDX2*, an intestine-specific transcription factor belonging to the *caudal*-related homeobox gene family, was involved in the induction of intestinal metaplasia of the stomach [45]. We have recently clarified the significant role of Sp1 in the basal transcriptional regulation of PEPT1 [46], but the mechanisms of intestine-specific expression of PEPT1 have not been clarified yet. CDX2 may also be responsible for the small intestinal and gastric expression of PEPT1.

Among organic ion transporters tested, only OCTN2 showed significant expression in the intestine, as the same expression level of PEPT1. The physiological substrate for OCTN2 is the carnitine, and mutations in this protein cause the autosomal recessive systemic carnitine deficiency [47]. In addition to carnitine, OCTN2 can transport various drugs such as verapamil [48]. This transport activity and abundant expression in the intestine suggested the pharamcokinetic role of OCTN2 for intestinal absorption like PEPT1. Using *Oct1* knockout mice, it was demonstrated that Oct1 plays important roles for intestinal excretion of cationic drugs [49]. But, the present expression analyses revealed that there was little expression of OCT1 along the digestive tract. Further studies are needed to clarify the clinical implication of intestinal OCT1.

In conclusion, we demonstrated the expression profile of PEPT1, amino acid transporters and organic ion transporters along the human digestive tract. The reciprocal distribution of PEPT1 and B^0AT1 may contribute to the efficient absorption of digestive products of ingested proteins. PEPT1 expression in the stomach is caused by intestinal metaplasia. OCTN2 is also abundantly expressed in the intestine. These findings may provide useful information about enteral nutrition, gastric pathology and pharmacology.

Acknowledgements

This work was supported by the 21st Century COE Program "Knowledge Information Infrastructure for Genome Science", a Grant-in-Aid for Research on Advanced Medical Technology from the Ministry of Health, Labor and Welfare of Japan, and a grant from the Astellas Foundation for Research on Metabolic Disorders.

References

[1] Adibi SA. The oligopeptide transporter (Pept-1) in human intestine: biology and function. Gastroenterology 1997;113:332–40.
[2] Daniel H. Molecular and integrative physiology of intestinal peptide transport. Annu Rev Physiol 2004;66:361–84.
[3] Terada T, Inui K. Peptide transporters: structure, function, regulation and application for drug delivery. Curr Drug Metab 2004;5:85–94.
[4] Christensen HN. Role of amino acid transport and countertransport in nutrition and metabolism. Physiol Rev 1990;70:43–77.
[5] Verrey F, Closs EI, Wagner CA, Palacin M, Endou H, Kanai Y. CATs and HATs: the SLC7 family of amino acid transporters. Pflugers Arch 2004;447:532–42.
[6] Verrey F, Ristic Z, Romeo E, Ramadam T, Makrides V, Dave MH, et al. Novel renal amino acid transporters. Annu Rev Physiol 2005;67:557–72.
[7] Stevens BR, Ross HJ, Wright EM. Multiple transport pathways for neutral amino acids in rabbit jejunal brush border vesicles. J Membr Biol 1982;66:213–25.
[8] Munck BG, Munck LK. Phenylalanine transport in rabbit small intestine. J Physiol 1994;480:99–107.
[9] Seow HF, Broer S, Broer A, Bailey CG, Potter SJ, Cavanaugh JA, et al. Hartnup disorder is caused by mutations in the gene encoding the neutral amino acid transporter SLC6A19. Nat Genet 2004;36:999–1002.
[10] Kleta R, Romeo E, Ristic Z, Ohura T, Stuart C, Arcos-Burgos M, et al. Mutations in SLC6A19, encoding B^0AT1, cause Hartnup disorder. Nat Genet 2004;36:1003–7.
[11] Motohashi H, Sakurai Y, Saito H, Masuda S, Urakami Y, Goto M, et al. Gene expression levels and immunolocalization of organic ion transporters in the human kidney. J Am Soc Nephrol 2002;13:866–74.
[12] Masuda S, Uemoto S, Goto M, Fujimoto Y, Tanaka K, Inui K. Tacrolimus therapy according to mucosal MDR1 levels in small-bowel transplant recipients. Clin Pharmacol Ther 2004;75:352–61.
[13] Ashida K, Katsura T, Motohashi H, Saito H, Inui K. Thyroid hormone regulates the activity and expression of the peptide transporter PEPT1 in Caco-2 cells. Am J Physiol Gastrointest Liver Physiol 2002;282: G617–23.

[14] Hashida T, Masuda S, Uemoto S, Saito H, Tanaka K, Inui K. Pharmacokinetic and prognostic significance of intestinal MDR1 expression in recipients of living-donor liver transplantation. Clin Pharmacol Ther 2001;69:308–16.
[15] Zimmermann C, Gutmann H, Hruz P, Gutzwiller JP, Beglinger C, Drewe J. Mapping of MDR1 and MRP1–5 mRNA expression along the human intestinal tract. Drug Metab Dispos 2005;33: 219–24.
[16] Mouly S, Paine MF. P-glycoprotein increases from proximal to distal regions of human small intestine. Pharm Res 2003;20:1595–9.
[17] Fojo AT, Ueda K, Slamon DJ, Poplack DG, Gottesman MM, Pastan I. Expression of a multidrug-resistance gene in human tumors and tissues. Proc Natl Acad Sci USA 1987;84:265–9.
[18] Ogihara H, Saito H, Shin BC, Terada T, Takenoshita S, Nagamachi Y, et al. Immuno-localization of H^+/peptide cotransporter in rat digestive tract. Biochem Biophys Res Commun 1996;220:848–52.
[19] Fenoglio-Preiser CM, Lantz PE, Listrom MB, Davis M, Rilke FO. Metaplasia. Gastrointestinal pathology: an atlas and text. New York: Raven, 1989. p. 154–7.
[20] Trejdosiewicz LK, Malizia G, Oakes J, Losowsky MS, Janossy G. Expression of the common acute lymphoblastic leukaemia antigen (CALLA gp100) in the brush border of normal jejunum and jejunum of patients with coeliac disease. J Clin Pathol 1985;38:1002–6.
[21] Kekuda R, Prasad PD, Fei YJ, Torres-Zamorano V, Sinha S, Yang-Feng TL, et al. Cloning of the sodium-dependent, broad-scope, neutral amino acid transporter B^0 from a human placental choriocarcinoma cell line. J Biol Chem 1996;271:18657–61.
[22] Feliubadalo L, Font M, Purroy J, Rousaud F, Estivill X, Nunes V, et al. Non-type I cystinuria caused by mutations in SLC7A9, encoding a subunit ($b^{0,+}$AT) of rBAT, International Cystinuria Consortium. Nat Genet 1999;23:52–7.
[23] Kanai Y, Segawa H, Miyamoto K, Uchino H, Takeda E, Endou H. Expression cloning and characterization of a transporter for large neutral amino acids activated by the heavy chain of 4F2 antigen (CD98). J Biol Chem 1998;273:23629–32.
[24] Mastroberardino L, Spindler B, Pfeiffer R, Skelly PJ, Loffing J, Shoemaker CB, et al. Amino-acid transport by heterodimers of 4F2hc/CD98 and members of a permease family. Nature 1998;395: 288–91.
[25] Pineda M, Fernandez E, Torrents D, Estevez R, Lopez C, Camps M, et al. Identification of a membrane protein, LAT-2, that co-expresses with 4F2 heavy chain, an L-type amino acid transport activity with broad specificity for small and large zwitterionic amino acids. J Biol Chem 1999;274:19738–44.
[26] Segawa H, Fukasawa Y, Miyamoto K, Takeda E, Endou H, Kanai Y. Identification and functional characterization of a Na^+-independent neutral amino acid transporter with broad substrate selectivity. J Biol Chem 1999;274:19745–51.
[27] Rossier G, Meier C, Bauch C, Summa V, Sordat B, Verrey F, et al. LAT2, a new basolateral 4F2hc/CD98-associated amino acid transporter of kidney and intestine. J Biol Chem 1999;274: 34948–54.
[28] Torrents D, Mykkanen J, Pineda M, Feliubadalo L, Estevez R, de Cid R, et al. Identification of SLC7A7, encoding y^+LAT-1, as the lysinuric protein intolerance gene. Nat Genet 1999;21:293–6.
[29] Sugawara M, Nakanishi T, Fei YJ, Huang W, Ganapathy ME, Leibach FH, et al. Cloning of an amino acid transporter with functional characteristics and tissue expression pattern identical to that of system A. J Biol Chem 2000;275:16473–7.
[30] Inui K, Masuda S, Saito H. Cellular and molecular aspects of drug transport in the kidney. Kidney Int 2000;58:944–58.
[31] Jonker JW, Schinkel AH. Pharmacological and physiological functions of the polyspecific organic cation transporters: OCT1, 2 and 3 (SLC22A1–3). J Pharmacol Exp Ther 2004;308:2–9.
[32] Adibi SA, Mercer DW. Protein digestion in human intestine as reflected in luminal, mucosal, and plasma amino acid concentrations after meals. J Clin Invest 1973;52:1586–94.
[33] Kim YS, Birtwhistle W, Kim YW. Peptide hydrolases in the bruch border and soluble fractions of small intestinal mucosa of rat and man. J Clin Invest 1972;51:1419–30.
[34] Crampton RF, Lis MT, Matthews DM. Sites of maximal absorption and hydrolysis of two dipeptides by rat small intestine in vivo. Clin Sci 1973;44:583–94.
[35] Schedl HP, Burston D, Taylor E, Matthews DM. Kinetics of mucosal influx of glycylsarcosine, glycine and leucine into hamster jejunum and ileum in vitro. Clin Sci (Lond) 1979;56:25–31.
[36] Munck LK, Munck BG. Variation in amino acid transport along the rabbit small intestine. Mutual jejunal carriers of leucine and lysine. Biochim Biophys Acta 1992;1116:83–90.
[37] Ganapathy V, Brandsch M, Leibach FH. Intestinal transport of amino acids and proteins. In: Johnson LR, editor. Physiology of the gastrointestinal tract. 3rd ed., New York: Raven; 1994. p. 1773–94.
[38] Das M, Radhakrishnan AN. A comparative study of the distribution of soluble and particulate glycyl-L-leucine hydrolase in the small intestine. Clin Sci Mol Med 1974;46:501–10.
[39] Terada T, Sawada K, Saito H, Hashimoto Y, Inui K. Functional characteristics of basolateral peptide transporter in the human intestinal cell line Caco-2. Am J Physiol 1999;276:G1435–41.
[40] Gutmann H, Hruz P, Zimmermann C, Beglinger C, Drewe J. Distribution of breast cancer resistance protein (BCRP/ABCG2) mRNA expression along the human GI tract. Biochem Pharmacol 2005;70:695–9.
[41] Litman T, Brangi M, Hudson E, Fetsch P, Abati A, Ross DD, et al. The multidrug-resistant phenotype associated with overexpression of the new ABC half-transporter, MXR (ABCG2). J Cell Sci 2000;113:2011–21.
[42] Dave MH, Schulz N, Zecevic M, Wagner CA, Verrey F. Expression of heteromeric amino acid transporters along the murine intestine. J Physiol 2004;558:597–610.
[43] Hellier MD, Holdsworth CD, Perrett D, Thirumalai C. Intestinal depeptide transport in normal and cystinuric subjects. Clin Sci 1972;43:659–68.
[44] Leung WK, Yu J, Chan FK, To KF, Chan MW, Ebert MP, et al. Expression of trefoil peptides (TFF1, TFF2, and TFF3) in gastric carcinomas, intestinal metaplasia, and non-neoplastic gastric tissues. J Pathol 2002;197:582–8.
[45] Yuasa Y. Control of gut differentiation and intestinal-type gastric carcinogenesis. Nat Rev Cancer 2003;3:592–600.
[46] Shimakura J, Terada T, Katsura T, Inui K. Characterization of the human peptide transporter PEPT1 promoter: Sp1 functions as a basal transcriptional regulator of human PEPT1. Am J Physiol Gastrointest Liver Physiol 2005;289:G471–7.
[47] Nezu J, Tamai I, Oku A, Ohashi R, Yabuuchi H, Hashimoto N, et al. Primary systemic carnitine deficiency is caused by mutations in a gene encoding sodium ion-dependent carnitine transporter. Nat Genet 1999; 21:91–4.
[48] Ohashi R, Tamai I, Yabuuchi H, Nezu J, Oku A, Sai Y, et al. Na^+-dependent carnitine transport by organic cation transporter (OCTN2): its pharmacological and toxicological relevance. J Pharmacol Exp Ther 1999;291:778–84.
[49] Jonker JW, Wagenaar E, Mol CA, Buitelaar M, Koepsell H, Smit JW, et al. Reduced hepatic uptake and intestinal excretion of organic cations in mice with a targeted disruption of the organic cation transporter 1 (Oct1 [Slc22a1]) gene. Mol Cell Biol 2001;21:5471–7.

Available online at www.sciencedirect.com
SCIENCE DIRECT®
Biochemical Pharmacology 70 (2005) 1823–1831
Biochemical Pharmacology
www.elsevier.com/locate/biochempharm

Association between tubular toxicity of cisplatin and expression of organic cation transporter rOCT2 (Slc22a2) in the rat

Atsushi Yonezawa, Satohiro Masuda, Kumiko Nishihara, Ikuko Yano, Toshiya Katsura, Ken-ichi Inui *

Department of Pharmacy, Kyoto University Hospital, Faculty of Medicine, Sakyo-ku, Kyoto 606-507, Japan

Received 26 August 2005; accepted 23 September 2005

Abstract

Cisplatin is an effective anticancer drug, but has its severe adverse effects, especially nephrotoxicity. The molecular mechanism of cisplatin-induced nephrotoxicity is still not clear. In the present study, we examined the role of rat (r)OCT2, an organic cation transporter predominantly expressed in the kidney, in the tubular toxicity of cisplatin. Using HEK293 cells stably expressing rOCT2 (HEK-rOCT2), we evaluated the cisplatin-induced release of lactate dehydrogenase and the uptake of cisplatin. The release of lactate dehydrogenase and the accumulation of platinum were greater in HEK-rOCT2 cells treated with cisplatin than in mock-transfected cells. Moreover, cimetidine and corticosterone, OCT2 inhibitors, inhibited the cytotoxicity and the transport of cisplatin in HEK-rOCT2 cells. Pharmacokinetics of cisplatin was investigated in male and female rats because the renal expression level of rOCT2 was higher in male than female rats. The renal uptake clearance of cisplatin was greater in male than female rats, while the hepatic uptake clearance was similar between the sexes. In addition, glomerular filtration rate and liver function were unchanged, but *N*-acetyl-β-D-glucosaminidase activity in the bladder urine and the urine volume were markedly increased 2 days after the administration of 2 mg/kg of cisplatin in male rats. Moreover, cisplatin did not induce the elevation of urinary *N*-acetyl-β-D-glucosaminidase activity in the castrated male rats whose renal rOCT2 level was lower than that of the sham-operated rats. In conclusion, the present results indicated that renal rOCT2 expression was the major determinant of cisplatin-induced tubular toxicity.

Keywords: Cisplatin; Organic cation transporter 2; Nephrotoxicity; Cytotoxicity; Renal tubular epithelial cells; Pharmacokinetics

1. Introduction

cis-Diamminedichloroplatinum II (CDDP, cisplatin) is widely used to treat solid tumors of prostate, bladder, colon, lung, testis and brain. Although cisplatin is an effective anticancer agent, severe nephrotoxicity limits its clinical application. It was reported that an increase in the serum creatinine concentration was observed in 41% of patients treated with high-dose cisplatin [1]. However, the major site of cisplatin-induced renal injury is the proximal tubule [2]. In addition, cisplatin induced tubular toxicity, followed by an increase in the serum creatinine level [3]. Moreover, the tubular toxicity caused a decrease in the glomerular filtration rate (GFR), resulting in acute renal failure [4]. Therefore, it was suggested that cisplatin was toxic primarily to renal tubular epithelial cells. But, the molecular mechanism of cisplatin-induced nephrotoxicity is still unknown.

Safirstein et al. [5] reported that cisplatin was concentrated in rat renal cortical slices five-fold above the concentration in medium. We previously demonstrated that cisplatin treatment from the basolateral side caused sever toxicity compared to the apical side in the porcine derived epithelial cell line LLC-PK_1 cells [6]. Recently, Ludwig et al. [7] reported that cisplatin-induced cytotoxicity was specifically observed from the basolateral side, and the toxicity was ameliorated in the presence of cimetidine in

* Corresponding author. Tel.: +81 75 751 3577; fax: +81 75 751 4207.
E-mail address: inui@kuhp.kyoto-u.ac.jp (K.-i. Inui).

0006-2952/$ – see front matter © 2005 Elsevier Inc. All rights reserved.
doi:10.1016/j.bcp.2005.09.020

Madin-Darby canine kidney (MDCK) cells. These reports suggested that the uptake of cisplatin in tubular epithelial cells was mediated by basolateral drug transporter(s). Identification of the transporter(s) is essential to understand the mechanism of cisplatin-induced nephrotoxicity.

Human organic cation transporter 2 (hOCT2) is the most abundant organic cation transporter in the kidney among an organic cation transporter family which consists of hOCT1-3 (SLC22A1-3) and hOCTN1 and 2 (SLC22A4 and 5) [8,9]. Rat (r)OCT2 is expressed predominantly in the basolateral membranes of proximal tubules and mediated the accumulation of various cationic drugs into proximal tubular epithelial cells from the circulation [10–14]. Uptake of tetraethylammonium (TEA) by rOCT2 was suppressed by the replacement of Na^+ with K^+, suggesting that the transport activity of rOCT2 was membrane potential-dependent [9, 15]. Based on such backgrounds and findings, we hypothesized that rOCT2 was the key molecule to clarifying the tubular accumulation and subsequent nephrotoxicity of cisplatin.

In the present study, we investigated whether rOCT2 affected the nephrotoxicity of cisplatin in rat proximal tubules. We examined the effect of rOCT2 expression on the cytotoxicity of cisplatin in HEK293 transfectants and on the pharmacokinetics of cisplatin in rats.

2. Materials and methods

2.1. Cell culture and transfection

HEK293 cells (American Type Culture Collection CRL-1573) were cultured in complete medium consisting of Dulbecco's modified Eagle's medium (Sigma Chemical Co., St. Louis, MO) with 10% fetal bovine serum (Whittaker Bioproducts Inc., St. Louis, MO) in an atmosphere of 5% CO_2–95% air at 37 °C.

The construction of HEK293 cells stably expressing rOCT2 (HEK-rOCT2) was performed as described [14]. The transfectants were used for the experiments at 48 h after seeding.

For a transient expression system, pBK-CMV plasmid vector DNA (Stratagene, La Jolla, CA), containing rOCT1 or rOCT2 cDNA, was purified using Wizard® Plus SV Minipreps DNA Purification System (Promega, San Luis Obispo, CA). The day before transfection, HEK293 cells were seeded onto poly-D-lysine-coated 24-well plates at a density of 2.0×10^5 cells per well. The cells were transfected with 50 ng of total plasmid DNA per well using 0.125 μl of LipofectAMINE 2000 (Invitrogen, Carlsbad, CA) per well according to the manufacturer's instructions. Forty-eight hours after the transfection, the cells were used for uptake experiments.

2.2. Uptake experiment

Cellular uptake of [^{14}C]TEA (88.8 MBq/mmol, Perkin-Elmer Inc., Wellesley, MA) was measured with monolayer cultures grown on poly-D-lysine-coated 24-well plates. The composition of the incubation buffer was as follows: 145 mM NaCl, 3 mM KCl, 1 mM $CaCl_2$, 0.5 mM $MgCl_2$, 5 mM D-glucose and 5 mM HEPES (pH 7.4 adjusted with NaOH). Experimental procedures were performed as described previously [14].

For the measurement of cisplatin uptake, seeded cells were incubated with the medium containing cisplatin with or without cimetidine or corticosterone for 1 h. After this incubation, the monolayers were rapidly washed twice with ice-cold incubation buffer containing 1% bovine serum albumin (Nacalai Tesque, Kyoto, Japan) and then washed three times with ice-cold incubation buffer. The cells were solubilized in 0.5N NaOH, and the amount of platinum was determined using inductively coupled plasma-mass spectrometry (ICP-MS) by the Pharmacokinetics and Bioanalysis Center, Shin Nippon Biomedical Laboratories, Ltd. (Wakayama, Japan).

The protein content of the cell monolayers solubilized in 0.5N NaOH was determined by the method of Bradford with a Bio-Rad Protein Assay Kit (Bio-Rad Laboratories, Richmond, CA).

2.3. Cytotoxicity experiment

The cytotoxicity of cisplatin was measured with monolayer cultures grown on poly-D-lysine-coated 12-well plates. Cells were incubated with the medium containing cisplatin with or without cimetidine or corticosterone for 2 h. After removal of the medium, drug-free medium was added. After incubation for 24 h, the medium was collected, and the lactate dehydrogenase (LDH) activity in the medium was measured using a LDH Cytotoxicity Detection Kit (Takara, Shiga, Japan), according to the manufacturer's instructions. Cytotoxicity was evaluated by measuring LDH activity in the medium. Total LDH activity was defined as LDH activity in the medium containing 1% TritonX-100. LDH release represents (LDH activity − LDH activity of control)/(total LDH activity − LDH activity of control).

2.4. Quantification of mRNA expression

Cellular total RNA was extracted using a MagNA Pure LC RNA isolation kit II (Roche Diagnostic GmbH, Mannheim, Germany) [8]. The total RNA was reverse-transcribed, and the single stranded DNA was used for the quantification of mRNA expression.

Real-time PCR was performed in a total volume of 20 μl containing 2 μl of reverse-transcribed cDNA, 1 μM forward and reverse primers, 0.2 μM TaqMan probe, and 10 μl of TaqMan Universal PCR Master Mix (Applied

Biosystems, Foster City, CA). The quantification of mRNA was performed as reported [8].

2.5. Pharmacokinetics of cisplatin

The pharmacokinetics experiment was performed using male or female Wistar/ST rats (8 weeks), as described previously with some modifications [16]. Cisplatin (0.5 mg/kg) was administered as a bolus via the catheterized right femoral vein. Blood samples were collected at 0.5, 1, 1.5, 2, 2.5 and 3 min from the left femoral artery. Three minutes after the injection, the kidney and liver were collected immediately after sacrificing the rats. The excised tissues were gently washed, weighed and homogenized in 3 volumes of 0.9% NaCl. The amounts of cisplatin were measured by ICP-MS. The animal experiments were performed in accordance with the "Guidelines for Animal Experiments of Kyoto University". All protocols were previously approved by the Animal Research Committee, Graduate School of Medicine, Kyoto University.

2.6. Western blot analysis

The crude membrane fractions were prepared from rat kidneys as described previously [17]. The crude membrane fractions (25 μg) were separated by 10% sodium dodecyl sulphate-polyacrylamide gel electrophoresis (SDS-PAGE) and transferred onto polyvinylidene difluoride membranes (Immobilon-P®, Millipore, Bedford, MA) by semi-dry electroblotting. The blots were blocked and incubated overnight at 4 °C with each primary antibody specific for rOCT2 [18], or the Na^+/K^+-ATPase α1 subunit (Upstate Biotechnology Inc., Lake Placid, NY). The bound antibody was detected on X-ray film using enhanced chemiluminescence (ECL) with horseradish peroxidase-conjugated secondary antibodies and cyclic diacylhydrazides (Amersham Pharmacia Biotech, Uppsala, Sweden).

2.7. Acute renal failure

Male Wistar/ST rats (8 weeks) were used or male rats (5 weeks) were surgically castrated 3 weeks before the experiment. Acute renal failure was induced by intraperitoneal administration of 2 mg/kg of cisplatin. Rats were maintained in metabolic cages for 24 h before the experiment to determine urine output and the urinary level of creatinine. Two days after the administration of cisplatin, plasma and bladder urine samples were collected and then the state of the kidneys was determined, as previously described [19]. The liver function data were determined using the assay kits from Wako Pure Chemical Industries (Osaka, Japan). The concentration of testosterone was measured using an ELISA kit (Cayman Chemical Co., Ann Arbor, MI).

2.8. Statistical analysis

Data are expressed as means ± S.E.M. Data were analyzed statistically using the unpaired Student *t* test. Multiple comparisons were performed with Dunnett's two-tailed test after a one-way ANOVA. Probability values of less than 0.05 were considered statistically significant.

3. Results

3.1. Uptake of TEA by HEK293 cells stably expressing rOCT2

We constructed HEK293 cells stably transfected with the pBK-CMV vector or rOCT2-containing vector (HEK-pBK or HEK-rOCT2). To check the function of these cells, the cellular uptake of [^{14}C]TEA by HEK-pBK cells or HEK-rOCT2 cells was measured. The amounts of [^{14}C]TEA in HEK-pBK cells and HEK-rOCT2 cells were 19.2 ± 4.0 and 317.4 ± 11.7 pmol/mg protein/2 min, respectively. Therefore, these cells were used in the subsequent experiments.

3.2. Cytotoxicity of cisplatin in HEK-pBK cells and HEK-rOCT2 cells

We compared the sensitivities of HEK-pBK cells and HEK-rOCT2 cells to cisplatin (Fig. 1). When HEK-pBK cells were treated with 30–300 μM cisplatin for 2 h and subsequently cultured in normal medium for 24 h, the release of LDH into the culture medium was not significantly enhanced. Treatment with 1000 μM cisplatin promoted the release of LDH in HEK-pBK cells. On the other hand, when HEK-rOCT2 cells were treated with 30–1000 μM cisplatin, the amount of LDH released increased in a dose-dependent manner. The release of LDH was greater in HEK-rOCT2 cells treated with 30–1000 μM cisplatin than in HEK-pBK cells (Fig. 1A). Further, we investigated the effects of OCT2 inhibitors, cimetidine and corticosterone, on the cisplatin-induced cytotoxicity. The cytotoxicity of cisplatin was completely inhibited in the presence of 1 mM cimetidine or 100 μM corticosterone in HEK-rOCT2 cells (Fig. 1B).

3.3. Transport of cisplatin by HEK-pBK cells and HEK-rOCT2 cells

To investigate whether rOCT2 recognizes cisplatin as its substrate, the effect of cisplatin on the uptake of [^{14}C]TEA and the accumulation of cisplatin by HEK-rOCT2 cells were examined (Fig. 2). Cisplatin, cimetidine and corticosterone had inhibitory effects on the uptake of [^{14}C]TEA by HEK-rOCT2 cells in a dose-dependent manner. The IC_{50} values of cisplatin, cimetidine and corticosterone were 2096.2 ± 59.5, 216.1 ± 4.5 and 2.50 ± 0.02 μM,

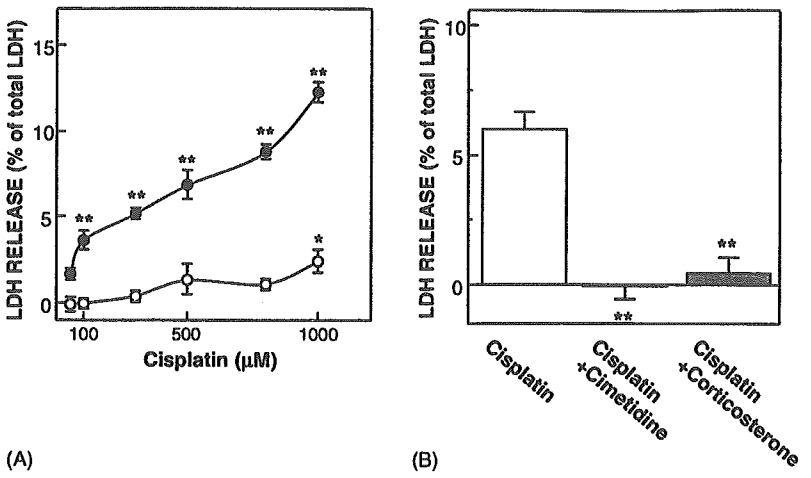

Fig. 1. Role of rOCT2 in the cytotoxicity of cisplatin. (A) Concentration-dependence of cytotoxicity in HEK-pBK cells (open circle) or HEK-rOCT2 cells (closed circle). Cells were exposed to cisplatin for 2 h, and then incubated in normal medium for 24 h. (B) Cimetidine (1 mM) or corticosterone (100 μM) was coadministrated with cisplatin (500 μM) for 2 h, and then the cells were incubated in normal medium for 24 h. Each point represents the mean ± S.E.M. of three wells. $^{*}P < 0.05$; $^{**}P < 0.01$, significantly different from control cells.

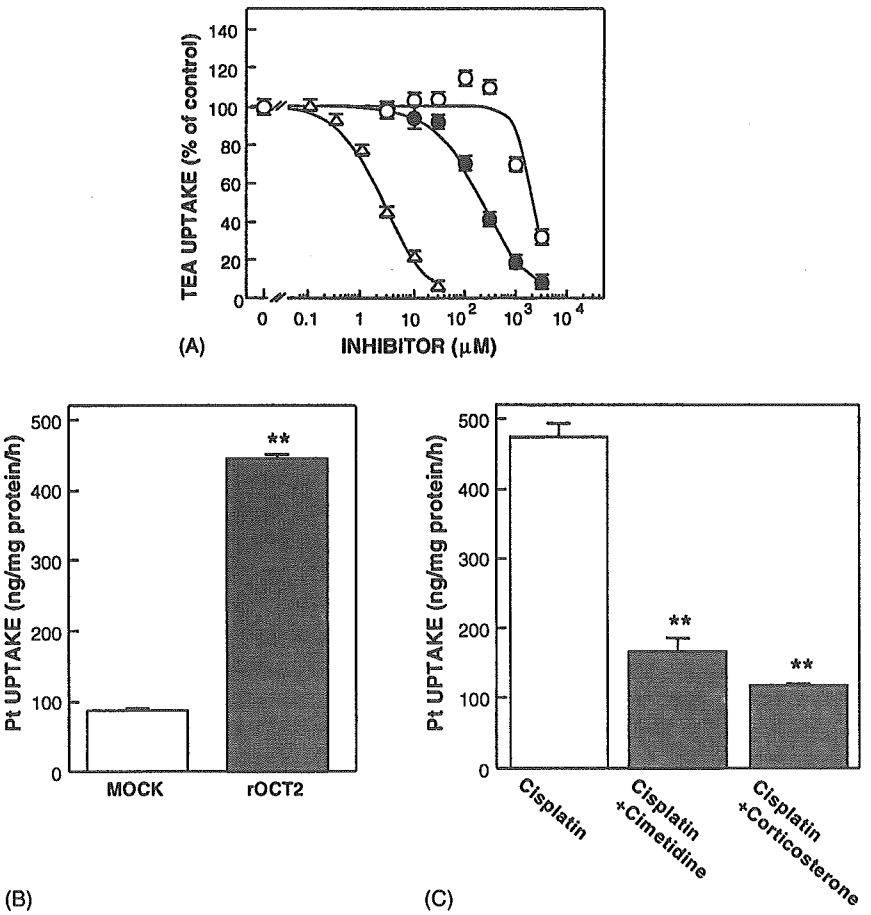

Fig. 2. Uptake of cisplatin by HEK-pBK cells or HEK-rOCT2 cells. (A) HEK-rOCT2 cells were incubated with 50 μM [^{14}C]TEA in the presence of cisplatin (open circle), cimetidine (closed circle) or corticosterone (open triangle) at various concentrations for 2 min. The amount of [^{14}C]TEA in HEK-rOCT2 cells was determined by measuring the radioactivity of solubilized cells. (B) HEK-pBK cells (MOCK) or HEK-rOCT2 cells (rOCT2) were incubated with 500 μM cisplatin for 1 h. (C) HEK-rOCT2 cells were incubated with 500 μM cisplatin in the presence or absence of 1 mM cimetidine or 100 μM corticosterone for 1 h. The amount of platinum in HEK-pBK cells or HEK-rOCT2 cells was determined by ICP-MS. Each point represents the mean ± S.E.M. of three or four wells. $^{**}P < 0.01$, significantly different from MOCK cells or control cells.